Contrib Mineral Petrol (2002) 142: 436–448
DOI 10.1007/s004100100298

Catherine Ginibre · Andreas Kronz · Gerhard Wörner

High-resolution quantitative imaging of plagioclase composition using accumulated backscattered electron images: new constraints on oscillatory zoning

Received: 25 October 2000 / Accepted: 8 July 2001 / Published online: 30 August 2001

Abstract Oscillatory zoning in plagioclase is investigated at small scale (≤10 μm) using accumulated backscattered electron (BSE) images as high-resolution imaging method. Combined with electron microprobe quantitative analysis, gray-value profiles across these images can be calibrated for An-content with a resolution of 0.5 mol% An. Applied to oscillatory-zoned crystals, this new application of BSE imaging allows better characterization of zoning patterns along a profile and quantification of wavelength, amplitude, and shape of the oscillations. We also obtain high-resolution information on the morphology of growth zones boundaries. This approach allows us to better classify the different types of "oscillations" and concentric zoning. Dissolution is more frequent than usually recognized. Major resorption surfaces crosscut several growth zones. Irregular 5–10-μm saw-tooth zones are delimited by faint wavy dissolution surfaces and must be distinguished from small-scale oscillations (≤1–3 μm) with straight boundaries. This suggests at least two mechanisms for the formation of these zoning patterns: faint oscillations are probably caused by local kinetic control whereas wavy dissolution surfaces involve magma chamber dynamics.

Introduction

One of the most spectacular zoning patterns in crystals consists of fine concentric euhedral zones of contrasting compositions, usually referred to as "oscillatory zoning". It is common in many igneous as well as hydrothermal minerals (Shore and Fowler 1996). The mineral most frequently investigated for oscillatory zoning is plagioclase because it is ubiquitous in igneous rocks and its zoning in anorthite content is readily observed under optical microscope. "Oscillatory zoning" in plagioclase is found in various volcanic rocks ranging in composition from basaltic (Anderson 1984; Kuritani 1998), to andesitic and rhyolitic (Nixon and Pearce 1987; Pearce and Kolisnik 1990; Singer et al. 1995) as well as in intrusive rocks (Wiebe 1968; Loomis and Welber 1982; Blundy and Shimizu; 1991; Brophy et al. 1996).

Zoning in plagioclase is characterized by changes in An-content, with variations generally ranging from 1 to over 30 mol% An. The analytical methods used to characterize this zoning in previous studies and their characteristics are summarized in Table 1. Quantitative profiles with analytical precision of ±1 mol% An at variable spatial resolution (≤3 μm) are obtained by electron microprobe (EMP) point analysis. Quantitative EMP analyses are also commonly used to calibrate the other quantitative methods, such as EMP X-ray profile of Ca, Na (Kuo and Kirkpatrick 1982; Loomis and Welber 1982; Smith and Lofgren 1983; Kuritani; 1998), and laser-interferometry (Nixon and Pearce 1987; Pearce et al. 1987; Pearce and Kolisnik 1990). Other techniques such as optical microscopy and Nomarsky interference contrast microscopy (NDIC) provide high-resolution images of zoning (Anderson 1983; Nixon and Pearce 1987; Pearce et al. 1987; Pearce and Kolisnik 1990; Singer et al. 1995). However, none of these methods combine two-dimensional morphological and quantitative compositional information. For this reason, most of the studies combine imaging (NDIC) and compositional measurement (EMP point analysis and/or laser interferometry). This has the disadvantage that the profile and the image have different spatial resolutions, which prevents an accurate correlation. As a result, very few studies quantitatively investigate in detail small-scale oscillations ≤10 μm in natural samples (Anderson 1984).

C. Ginibre (✉) · A. Kronz · G. Wörner
GZG, Abteilung Geochemie, Goldschmidtstr. 1,
37077 Göttingen, Germany
E-mail: cginibr@gwdg.de

Editorial responsibility: T.L. Grove

Table 1 Comparison of methods used for the characterization of compositional zoning in plagioclase

Method	Imaging	Quantitative analysis
Optical microscopy	Good contrast; spatial resolution of about 1 μm; for details varying with depth, the limiting factor is the thickness of the thin section (30 μm)	Differences of 1–2 mol% An can be measured. However, the values are determined for each zone. No continuous profiles can be obtained
Electron microprobe quantitative analysis	Quantitative mapping would be time-consuming and is never used	Profiles: spatial resolution generally coarser than 5 μm. Compositional resolution: 1% An
Nomarski differential interference contrast	Imaging of the surface. Very good contrast, spatial resolution comparable to that of optical microscopy. The image is sensitive to etching process and to the state of the surface before etching	No quantitative information
Laser interferometry	2-D information given by parallel profiles (interference fringes)	Profiles must be calibrated using EMP quantitative analyses. Resolution: 2 μm, 2.5 mol% An
Wavelength dispersive spectrometry profile (Ca)	Mappings are time-consuming and have lower spatial resolution than other imaging methods, rarely used to characterize plagioclase zoning	Profiles must be calibrated using EMP quantitative analyses. Resolution: 2–5 μm, 1–2 mol% An
Backscattered electron imaging	Imaging of the surface of the sample (1 μm). The signal/background ratio of normal BSE images is low but can be improved by accumulating several images of the same part of the sample. Spatial resolution: 0.5 μm	Profiles must be calibrated using EMP quantitative analyses. Compositional resolution $\leq$ 0.5 mol% An. The quantitative information is two-dimensional so that profiles may be directly compared with the zone morphology

Most studies distinguish irregular or rounded resorption surfaces, often correlated between different crystals (Loomis and Welber 1982), from euhedral oscillatory zoning, which cannot be correlated between crystals. Many authors attempted to interpret zoning in plagioclase in terms of processes that occur in the magma chamber (see reviews in Pearce 1994; Shore and Fowler 1996).

Major resorption surfaces are generally attributed to profound changes in temperature, pressure, melt composition, and water content in the magma at large scale caused, for example, by magma recharge (Nixon and Pearce 1987; Davidson and Tepely 1997). Minor resorption surfaces are attributed to local effects of minor changes in the same parameters caused by magma dynamics (convection). "Oscillatory zoning" is generally attributed to local kinetic effects in a boundary layer at the crystal–melt interface. Dynamic effects and recharge processes are generally well accepted, although rates and details of such processes are still poorly understood. Kinetic effects are even more difficult to constrain and have been theoretically and numerically modeled (Haase et al. 1980; Allègre et al. 1981; Lasaga 1982; Loomis 1982; Ortoleva 1990; L'Heureux and Fowler 1994; Wang and Wu 1995; L'Heureux and Fowler 1996a, 1996b). Other interpretations involve the periodic destruction of this boundary layer (Loomis 1982; Anderson 1984). Numerous experimental studies of plagioclase equilibria (Yoder et al. 1957; Johannes 1978; Housh and Luhr 1991) and growth kinetics (Lofgren 1974, 1980; Kirkpatrick et al. 1979; Muncill and Lasaga 1987, 1988) have been performed and used to explain zoning patterns. Oscillations in experimentally grown plagioclase are described in one single run of Lofgren's experiments (1980). These are faint oscillations (1–2 μm/1–2% An) and are also interpreted as being a result of kinetic control.

Despite this abundant literature on the topic, the interpretation of oscillatory zoning remains controversial. One reason is the lack of an unequivocal definition of oscillatory zoning. It appears that each author uses the term in a different sense and there is consensus neither on the shape, nor on the wavelength and amplitude of the variation. Whereas some authors (e.g. Smith and Brown 1988) consider only periodic oscillations on a micrometer scale, others consider that these oscillations "need not need to be regular or harmonic" (Shore and Fowler 1996). Between these extremes, authors describe or model more or less regular "oscillations", ranging from 1–5 μm and 1–2 mol% An to 10–100 μm and 5–15 mol% An. The shape of many profiles described consists mostly of asymmetrical variations or "saw-tooth patterns".

These problems in defining oscillatory zoning are probably caused by (1) the variability of such zoning patterns in plagioclase and in other minerals, and (2) the analytical difficulty in characterizing small-scale zoning patterns. A good characterization of natural zoning should provide (1) high-resolution quantitative An profiles to be compared with An profiles calculated by numerical models, and (2) two-dimensional information that shows the morphology of the zones, which may help to distinguish possible resorption surfaces from growth zones. None of the techniques discussed above satisfies both conditions together.

The present study demonstrates that accumulated BSE images provide a powerful quantitative imaging tool for plagioclase major element zoning. The spatial

resolution is ≤1 μm and thus equivalent to or even better than other imaging methods (NDIC). Furthermore, gray scales of such BSE images can be calibrated in terms of An content. The compositional resolution can be as small as 0.5 mol% An. The quantitative profiles obtained can be compared directly with the two-dimensional information.

This approach has been used here to study zoning patterns in a typical "oscillatory-zoned" plagioclase (andesine) from a dacite (Parinacota volcano, Chile). We will refine the classification between small-scale oscillations and larger-scale resorption events (Pearce and Kolisnik 1990), and provide a tool to better understand magma chamber processes. We distinguish (1) low amplitude oscillations that are possibly true periodic oscillations, (2) saw-tooth patterns, which make up most of the usually described "oscillatory zoning", and (3) major resorption surfaces. The newly defined zoning types can be better interpreted in terms of responsible dynamic and kinetic processes, as recorded in the growing crystals. The other sample studied here is a cumulate plagioclase from a phonolitic magma chamber (Laacher See, Eifel, Germany). It shows only low-amplitude oscillations, probably from kinetic controls.

We will first present our samples, techniques and results and then compare them to the existing model for oscillatory zoning and discuss the relevance of these models for zoning patterns of plagioclase in natural systems.

Samples

Dacite from the Parinacota volcano

Parinacota volcano (north Chile) belongs to the Central Volcanic Zone of the Andes and has been investigated by Wörner et al. (1988), Davidson et al. (1990), and Wörner et al. (2000). It consists of a Pleistocene to Recent calc-alkaline stratocone with compositions ranging from basaltic andesites to rhyodacites. We chose a dacite from a "Old Cone" lava dome (PAR-130, see Wörner et al. 1988) for our investigation. The mineralogy consists of plagioclase, amphibole, two pyroxenes, rounded biotite, and Ti–Fe oxides in a groundmass of glass with microliths of pyroxene, plagioclase and alkali-feldspar. Plagioclase phenocrysts have compositions ranging from An_{25} to An_{55}. The phenocryst population consists of two types. The majority comprises 1–2 mm large crystals showing oscillatory zoning throughout the crystal with only few resorption zones. Some smaller crystals show, in addition, several more extensive resorption zones. The crystal investigated here (PAR-130-P3) is representative of the large oscillatory zoned phenocrysts. Between various crystals of this type, however, we did not observe an obvious correlation of individual zones.

Syenite cumulate from the Laacher See

The Laacher See Tephra (Eifel, Germany) consists of 6.3 km^3 mafic to highly differentiated phonolite erupted 12.9 ka ago and represents an inverted zoned magma chamber (Wörner and Schminke 1984a, 1984b; Bogaard 1995; Harms and Schminke 2000). Late in the eruption, crystal-rich "nodules" were ejected. These cumulates are interpreted by Tait (1988) and Tait et al. (1989) as the crystallized wall of the magma chamber. Compositions range from mafic (pyroxene + amphibole) to felsic (syenite cumulates). Oscillatory zoning in plagioclase crystals is very rare in these cumulates. Sample 15616 in one of the few where fine oscillatory zoning is present in plagioclase. It belongs to group 1-intermediate-type 2 of Tait (1988) and contains two feldspars, pyroxene, and amphibole, and small amounts of interstitial glass. The investigated crystal is shown in Fig. 1. The core is extensively patchy zoned, similar to crystals found in the Laacher See pumices, and may have crystallized before accumulation. However, the rim, intergrown with other crystals (pyroxene, plagioclase), must have crystallized in situ. This rim is strongly normally zoned with weak superimposed oscillations, which can be seen under the optical microscope.

Analytical techniques

All analyses were performed on a JEOL 8900 RL electron microprobe at Göttingen. Zoning patterns were documented by backscattered electron (BSE) images. Details of the technique are given in the Appendix. The accumulation of several images of the same area of the

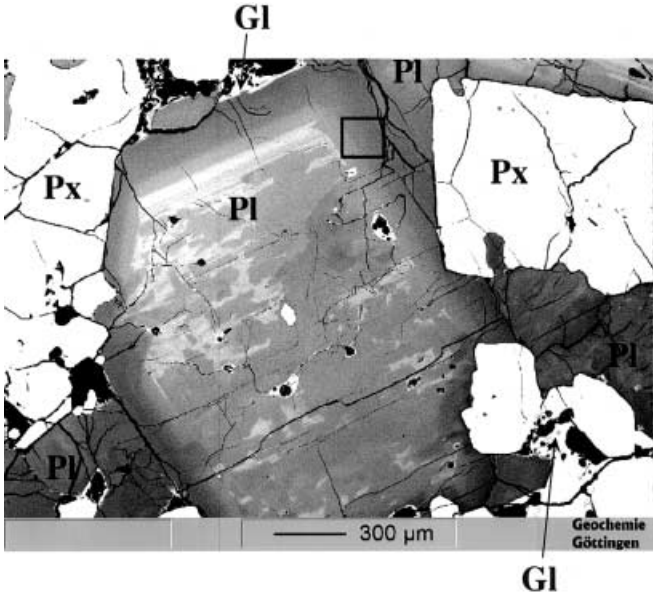

Fig. 1 BSE image of the cumulate LS 15616 showing the analyzed plagioclase crystal P1. The *box* indicates the location of the high-resolution image (Fig. 2)

sample increases the signal/noise ratio. Quantitative point analyses of major elements are used to calibrate the gray scale of the BSE-images in terms of An content. An example of the high-resolution BSE image and An-calibrated profiles is shown in Fig. 2 for the Laacher See sample (LS 15616). Gray scale profiles with superimposed EMP quantitative point analysis are given in Fig. 3 for the Parinacota dacite (PAR 130-P3).

The images and resulting profiles have a compositional resolution down to 0.5 mol% An and a spatial resolution down to 0.5 μm. Characteristics of BSE images are compared with other analytical techniques in Table 1. This shows that our approach is the only method that allows quantitative two-dimensional documentation of the plagioclase zoning pattern with such a spatial and compositional resolution at the scale of interest.

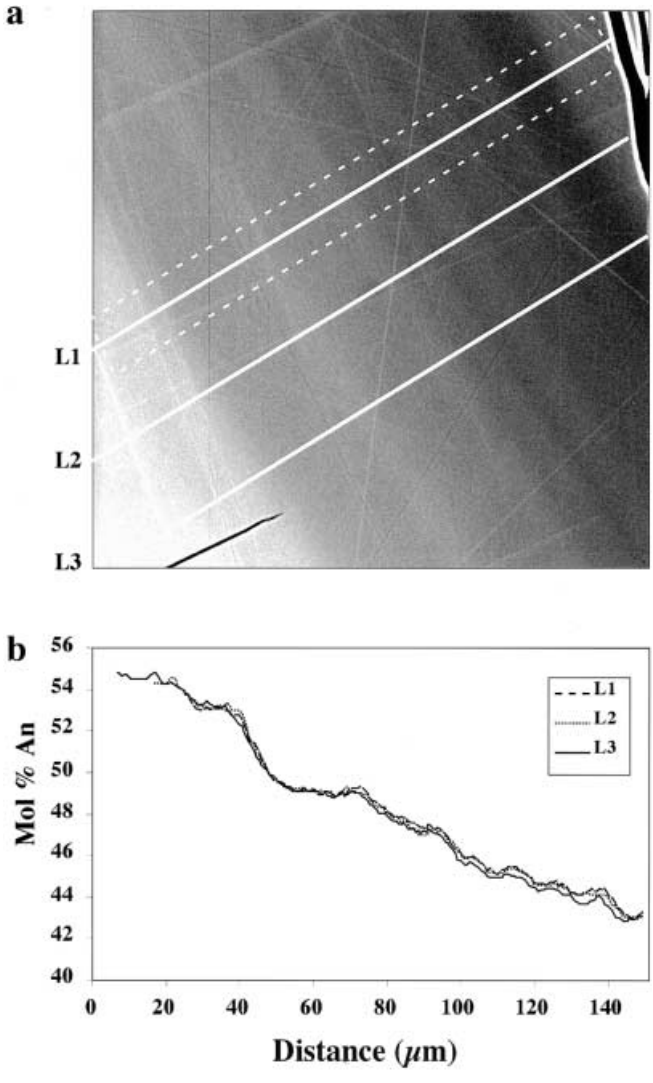

Fig. 2 **a** High-resolution BSE image and **b** corresponding An-calibrated gray scale profiles of crystal LS15616P1. Despite polishing artifacts, small-amplitude oscillations (0.5% An) are seen both on the image and the three parallel profiles. Sampling width (100 pixels) of the profiles is shown on L1 (*white dashed line*)

Results: "oscillatory" zoning patterns

The diversity of zoning patterns is seen in the phenocrysts from dacite PAR-130. One type (low amplitude oscillations) is particularly well seen in the rim of the cumulate crystal LS15616-P1.

Dacite PAR-130

Crystal PAR-130-P3 is shown as a BSE image in Fig. 3 along with a quantitative An profile and an An-calibrated gray scale profile from the accumulated BSE images. These accumulated images and corresponding profiles are shown in detail in Fig. 4a, b. Comparison of the detailed An profile with the two-dimensional image shows various types of zoning patterns as described below.

A few major resorption surfaces (R) are observed, which cross cut several 5- to 50-μm-wide growth layers at the corners of the growing crystal. They are characterized by wavy, highly irregular layers of up to 5 μm width, which are richer in An by 5–10 mol%. These are similar to those obtained in dissolution experiments of plagioclase (Tsuchiyama 1985; Johannes et al. 1994; Nakamura and Shimakita 1998; Hammouda and Pichavant 2000). However, compositional discontinuities

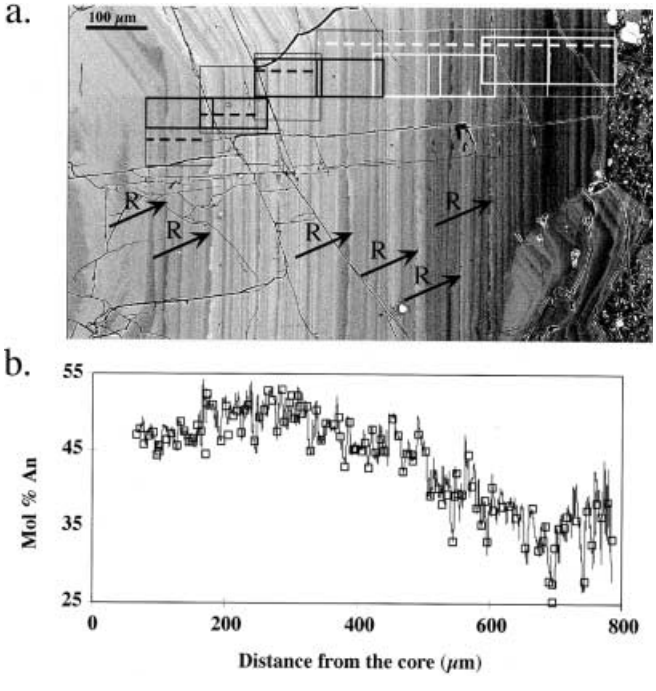

Fig. 3 **a** BSE-image of plagioclase crystal PAR-130-P3. Major resorption surfaces are indicated by *arrows*. *Dashed lines* show the location of quantitative profiles, *thin-lined boxes* represent the location of the accumulated BSE images and *thick-lined boxes* the part of the images shown in Fig. 4. **b** An-calibrated gray scale profile (*line*) and quantitative point analyses (*squares*). Details of the gray scale profile are shown in Fig. 4a, b

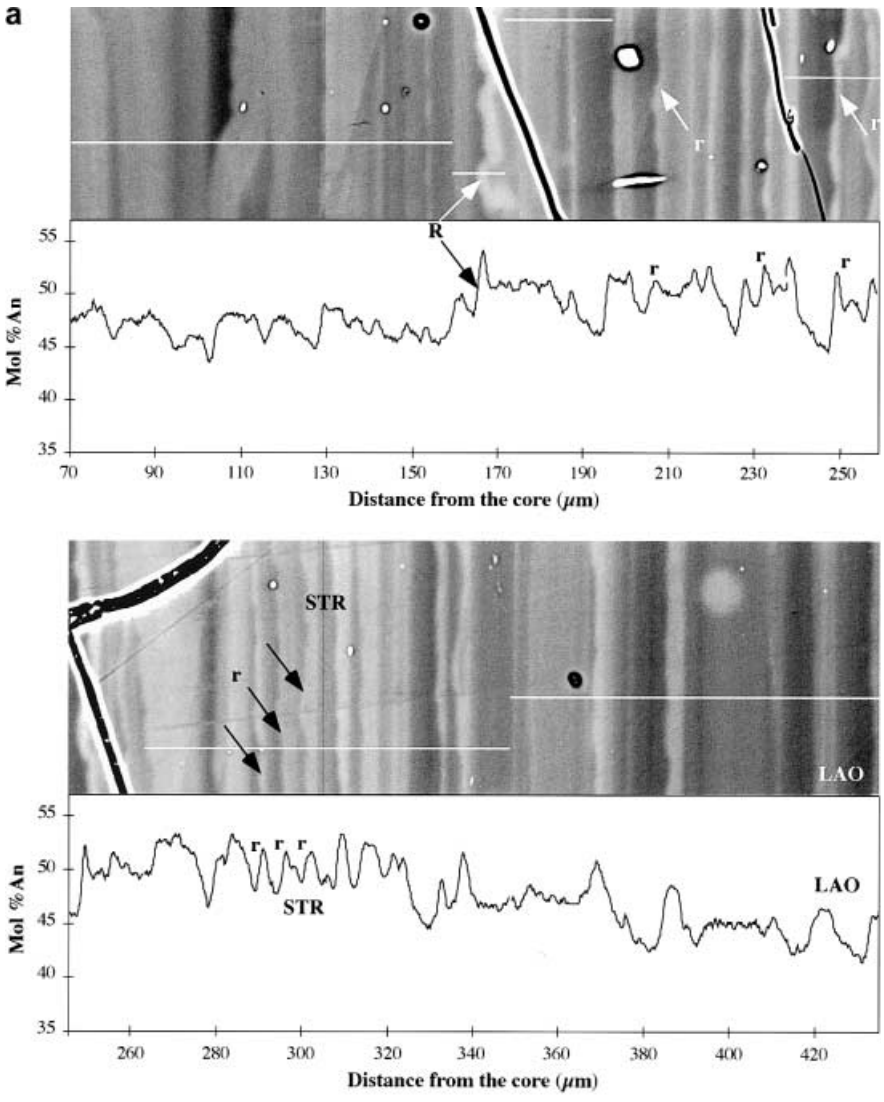

Fig. 4 **a** High-resolution BSE images and corresponding An-calibrated gray scale profile of PAR-130-P3. Examples for the features described in the text are indicated on the images and on the profiles. Major resorption surfaces (*R*) with calcic overgrowth is best seen at 170 μm. Minor resorption surfaces (*r*) separates individual normal zones in saw-tooth patterns (*STR*). The STR present on this part of the profile are very narrow (5 μm) and thus not typically asymmetrical. Small-amplitude oscillations (*LAO*) are seen at 420 μm. **b** High-resolution BSE images and corresponding An-calibrated gray scale profile of PAR-130-P3 continued. The comparison of two parallel profiles between 510 and 610 μm show the lateral variability of the profiles. Typical STR pattern with superimposed LAO is seen between 610 and 680 μm. High-frequency, high-amplitude An variations (*HFA*) with wavy zone boundaries occur in the outermost 20 μm grown during eruption

in crystals from PAR-130 never exceed 10 mol% An, in contrast with discontinuities of up to 30 mol% An, which are reported in the literature (Nixon and Pearce 1987; Singer et al. 1995) in other natural samples.

The most striking zoning pattern is a Saw-Tooth pattern with Resorption (STR): this pattern consists of repeated, mostly normally zoned growth layers, 5–20 μm wide, separated by wavy boundaries followed by a sharp increase in An. They are generally slightly rounded at the crystal edges. A thin calcic line is often present at the zone boundary and resembles that observed at major resorption surfaces. All these features indicate that these zone boundaries are in fact resorption surfaces. However, most of them represent only a minor resorption event (r in Fig. 4) because they affect only one growth layer. The resulting An profile shows peaks that are dominantly asymmetrical, and only some of the smallest peaks (in both width and An content) are almost symmetrical.

Some growth layers at the same scale of 5–10 μm are inversely zoned forming a saw-tooth pattern in the opposite sense (i in Fig. 4). The contact with the previously grown zone is sharp and straight, suggesting simple continued growth.

Superimposed on the normal zones of STR, faint repeated variations (≤2 mol% An, ≤1–5 μm) with straight boundaries are recognized as Low Amplitude Oscillations (LAO), both on the profile and on the image. Amplitude and wavelength are close to the analytical resolution and, thus, it is not possible to determine whether these variations are truly periodic. However, they seem more regular and periodic than STR and they are, therefore, considered as possible true oscillations in the following discussion.

The outermost 20 μm exhibit High-Frequency (3 μm in wavelength), high-Amplitude (10 mol% An) oscillations (HFA). Although narrower, they are very similar to the STR type with a similar amplitude (5–8 mol% An) and a sharp wavy boundary, as well as very fine superimposed oscillations (LAO) within individual zones. Again, recognition of the exact shape of the An profile is limited by the short wavelength, close to the

Fig. 4b (Contd.)

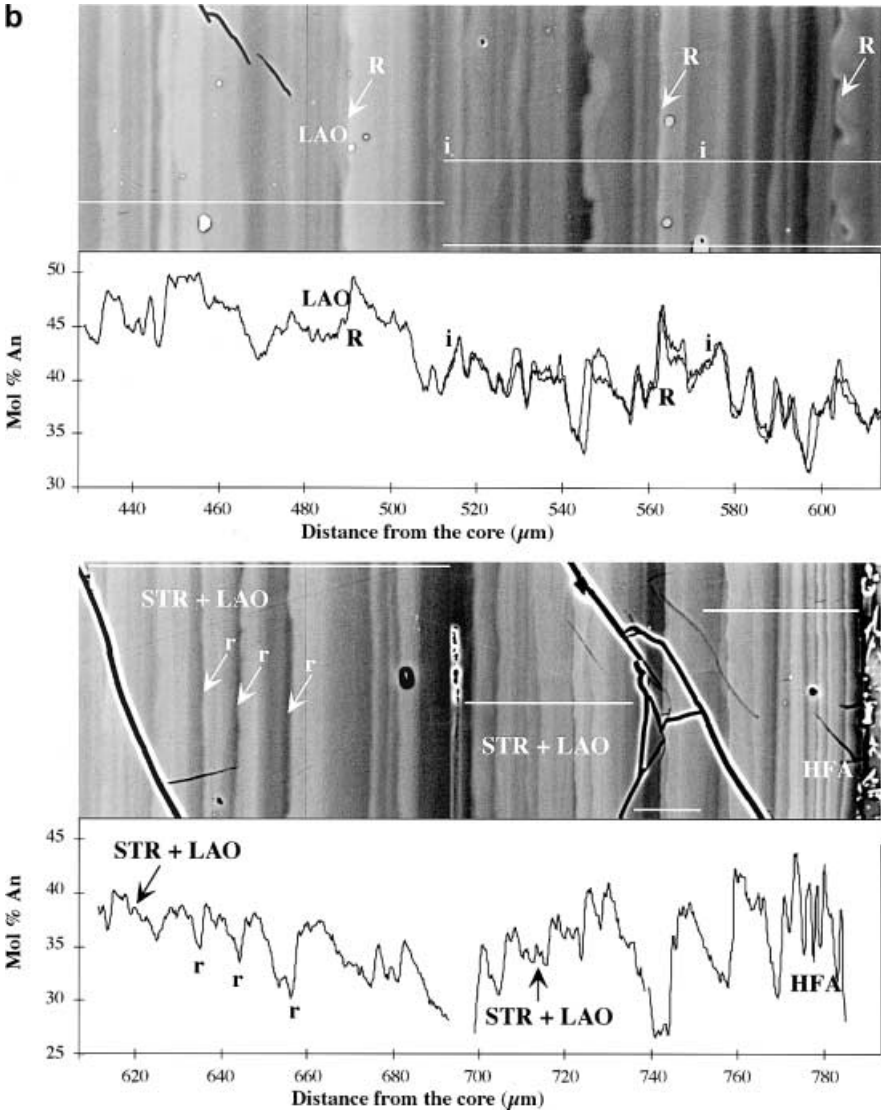

spatial resolution. We interpret these zones as a special case of STR, which is restricted to syn-eruption fast growth (see Discussion).

Cumulate LS15616

Low-amplitude (0.5 mol% An) oscillations (LAO) are also found in the rim of the plagioclase crystals of cumulate sample LS15616, but with a larger wavelength (10–20 μm) than in PAR-130 P3 (Fig. 2). Zone boundaries are straight and transitions are smooth. These oscillations are superimposed on a strong normal zoning (from An_{55} to An_{43}). Again, the shape of the oscillations is not clearly defined because of the low signal/noise ratio. In order to better characterize the nature of these oscillations, we considered the residual signal obtained by subtracting the profile, averaged over 20 μm (wavelength of the oscillations), from the initial profile. The result is shown in Fig. 5a. The wavelength of the oscillations decreases slightly toward the rim. Fourier analysis of the residual profile between 60 and 140 μm (Fig. 5b) shows two clear wavelengths at 21.2 and 10.6 μm. These zoning patterns can therefore be regarded as true oscillations.

Discussion

The zoning patterns observed here are similar to oscillations described in the literature (Pearce and Kolisnik 1990). They include normal and inverse saw-tooth patterns (STR) with 10–20 μm width and 5–10% An amplitude, and low amplitude oscillations (LAO) with 1–20 μm wavelength and 0.5–2 mol% An amplitude. Large discontinuities in the An profile, with up to 30–40 mol% An contrast (Nixon and Pearce 1987) and large patchy resorbed zones are absent in our samples. Both types (STR and LAO) are present within a single crystal from the Parinacota dacite. By contrast, the rim of the crystal from the Laacher See cumulate shows only LAO, which have two superimposed wavelengths, which are larger than in PAR-130-P3 (21.2 and 10.6 μm).

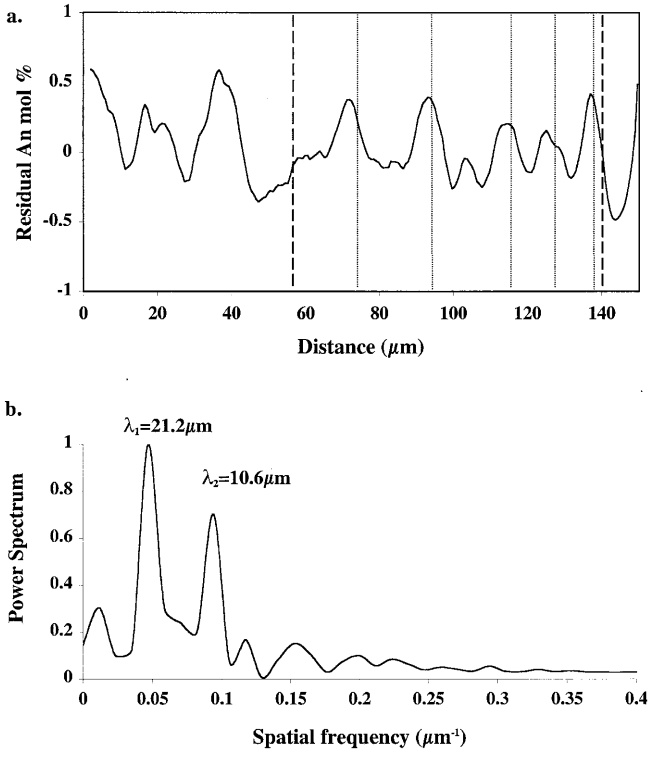

Fig. 5 **a** Residual An profile of the crystal from LS515616: the profile was smoothed by averaging the values over 20 μm and then subtracted from the original signal. The resulting profile was also smoothed by averaging over 2 μm in order to reduce the noise. **b** Normalized power spectrum of the residual profile obtained by fast Fourier transform. Two distinct wavelengths are recognized both on the profile and on the power spectrum

Accumulated BSE images allow one to identify many more resorption surfaces than are usually recognized, separating zones as narrow as 5 μm. Only Nixon and Pearce (1987) describe minor resorption surfaces every 10–20 μm. We found possible true oscillations without resorption only with very low amplitude (LAO).

A similar classification between small- and large-scale oscillations was made by Pearce and Kolisnik (1990) in a larger range of rock types. They distinguish small-scale oscillations (type I), which they attribute to kinetic effects, from larger oscillations that show resorption (type II) caused by changes in the bulk melt (temperature, composition, etc). However, their type I generally has saw-tooth-shaped profiles and ranges in composition from < 1 to 10% An, which typically overlaps the range of our STR patterns. Therefore, we suspect that their classification and interpretation may have overlooked dissolution surfaces in type-I oscillations because of a poorer resolution of the imaging method. We now discuss the relevance of theoretical models for the types of zoning that we observed. We will show that kinetic models do not apply to the most striking STR-patterns. LAO-patterns, however can be explained by some kinetic models whereas others are clearly inadequate.

In the recent literature on oscillatory zoning, there seems to be a consensus to explain planar "oscillatory" zoning by local kinetic effects and to try to develop the best numerical model for these oscillations. Several experimental (Lofgren 1974, 1980; Kirkpatrick et al. 1979; Muncill and Lasaga 1987, 1988) and theoretical (Kirkpatrick 1981; Baronnet 1984; Cashman 1990) studies have shown the importance of kinetics in growth processes. Crystal growth rate depends on melt supersaturation or undercooling at the crystal–melt interface. When the system is sufficiently undercooled with a correspondingly high crystal growth rate, element diffusion is too slow to replenish the melt at the interface. A chemical boundary layer then develops, where the supersaturation is lower than in the bulk melt. This influences the composition of the growing crystal. Kinetic models of oscillatory zoning are based on this competition between interface and diffusion kinetics (see review in Pearce 1994). These models, however, never imply resorption because the melt is always saturated in plagioclase. Because resorption at the scale of STR zoning patterns (5–20 μm) has rarely been recognized in previous studies, thermodynamic models that include repeated destabilization of the plagioclase to explain such oscillations have been rejected by most authors.

Our observations now show that "oscillatory zoning" in plagioclase is very variable in style and cause, and, therefore, must be classified as at least two different types: STR and LAO. Kinetic numerical models up to now have considered observed "oscillations" of 1 to 10% An in amplitude and 1 to 100 μm in wavelength, which apparently includes both STR and LAO types. However, STR "oscillations" are not true oscillations and exhibit evidence for repeated resorption at a scale as small as 5–20 μm. Therefore, they cannot be explained by existing kinetic models, which produce periodic oscillations and consider only growth. Models for STR zoning patterns should include resorption and produce non-periodic variations. Such kinetic models are presently not available. In contrast, LAO zoning may represent true oscillations for which kinetic models in fact exist because they have a regular wavelength and do not show observable resorption. Furthermore, LAO patterns also occur in crystals grown in a quiescent environment (cumulates) or superimposed on STR patterns, thus favoring local kinetics over external thermodynamic control.

We now discuss first dynamic models for STR and related HFA patterns, and then models that involve local kinetic models for LAO zoning patterns. The model of Loomis (1982), which involves both local kinetic and dynamic effects, is discussed for the interpretation of the inverse zoning.

Saw-tooth patterns: equilibrium models and magma chamber dynamics

Equilibrium models assume that the growing crystal is in equilibrium with the surrounding melt. The dependence of crystal composition on the physical (P, T) or com-

positional (water content, magma composition) parameters is determined by phase equilibria. Several studies have shown their influence on An content of the crystal (Yoder et al. 1957; Johannes 1978; Loomis and Welber 1982; Housh and Luhr 1991). Housh and Luhr (1991) investigated intermediate compositions and obtained a slope of the solidus of around 5 °C/% An.

Mechanisms thought to cause repeated changes in the environment of a growing crystal involve magma chamber dynamics. (1) Repeated magma recharge results in temperature increase, followed by composition changes if mechanical and chemical mixing is sufficient. (2) Gradients in temperature and composition are expected in magma chambers, at least in the thermal/chemical boundary layer (Marsh 1989). Movement of the crystals along these gradients by convection can produce periodic changes in T, water content, bulk composition, and, to a lesser extent, P, depending on the scale of the convection.

The latter mechanism was proposed by Homma (1932) to explain oscillatory zoning and has been invoked more recently by some authors to explain repeated minor (Singer et al. 1995) or major (Pearce and Kolisnik 1990) resorption surfaces. In contrast, large and prominent resorption with An variations of up to 40% (Singer et al. 1995; Davidson and Tepley 1997) are generally related to major magma chamber recharge events. We will show below that medium, non-periodic STR "oscillations" and their related small-scale resorption interfaces considered here can not be explained by magma recharge.

In sample PAR-130, STR "oscillations" exhibit resorption interface at only 5-to 10-μm spacing. The dependence of plagioclase composition on pressure is small. Any pressure changes, for example caused by to convection in typical magma chambers below stratovolcanoes, may reach 1 kb at most. This limits the effect of pressure. The most plausible cause for resorption is, therefore, thermal and compositional changes. For the observed variations in An concentration (compositional shift $\leq$ 5 mol% An), the temperature dependence of An reported above would imply temperature differences of only 5–25 °C.

If magma recharge were responsible for the STR oscillations, then there would have to be hundreds of small recharge events regularly timed during the growth time of any plagioclase crystal with only minor changes in the melt composition. This is inconsistent with conventional wisdom on the rate and volume of magma recharge events (Nixon and Pearce 1987; Davidson and Tepley 1997).

High-frequency, small temperature changes imply, at a local scale, mixing, crystal dispersion, or the effect of a thermal or compositional gradient. This is consistent with the results of the trace element study in the same crystal (Ginibre et al. 2001), which also argue for local mixing. One possible process for this is convection within the magma chamber. Laminar convection has been suggested as an explanation of repeated minor resorption by Singer et al. (1995). For 100-μm-spaced resorption surfaces, they calculate that this could occur in laminar convection cells of 100 m diameter. Their calculations applied to 10-μm-spaced resorption would give 10-m convection cells, which may be too small. In addition, laminar convection may not allow sufficient mixing. The observation of "R"-type resorption surfaces and STR oscillations suggests that both are dynamically controlled, the width of the zones being related to the nature and scale of convection.

The HFA oscillations at the rim of the crystal correspond to the last phase of crystallization, during or after eruption, where rapid growth rates are expected. Kinetic processes will thus play a more important role there. However, the repeated resorption surfaces that suggest a dynamical origin of STR-type are also present in HFA, suggesting a similar process. The narrower spatial scale at presumed higher growth rates indicates much shorter time-scales. If this interpretation is correct, an increase in the turbulence of the magma prior and/or during magma ascent and eruption could explain more rapid movements and changes in the magma composition and temperature at the contact of the crystals.

In contrast to the complex resorption-rich zoning of plagioclase from lavas, plagioclase crystals from Laacher See cumulates are characterized, at least in their outer part, by the absence of saw-tooth patterns and evidence of resorption. This is consistent with the absence of convection expected in the more quiescent environment where crystals accumulate. An alternative explanation could be that initial zoning patterns of higher amplitude, such as STR, have been almost completely erased by diffusion in the crystal. However, we observed these low amplitudes in the outer 200 μm of the crystal whereas larger contrasts are seen in the core. Furthermore, the time needed to compositionally equilibrate 20-μm-wide zones is $>10^4$ years at 1,100 °C (Grove et al. 1984). It would be at least two orders of magnitude larger at the temperature of phonolite ($<$ 880 °C, Wörner and Wright 1984, Berndt et al. 2001). This is much longer than the time estimated for the whole history of the Laacher See volcano (Tait et al. 1989; Bourdon et al. 1994).

Low-amplitude oscillations: kinetic models

Before discussing the relevance of the models we would like to draw attention to two points. First, all kinetic models assume a boundary layer at the crystal–melt interface, which necessitates a sufficiently high crystal growth rate and thus sufficient undercooling. However, the undercooling of natural magmas is not well constrained but is likely to be rather small (Cashman 1990). The existence of a boundary layer at the crystal–melt interface has been reported by Bottinga et al. (1966) in plagioclase-bearing basalt. However, this occurs in an erupted lava and it is not clear whether this gradient existed over the whole crystallization history of the

crystal, or was formed only during eruption and rapid cooling. Second, as shown above, models that involve kinetics should be designed to only explain LAO patterns and this restricts the range of amplitudes and wavelengths expected to be reproduced by the models. This is important because oscillations may be obtained in many non-linear dynamical models that consider different parameters (e.g., undercooling, partition coefficient) with variable values. Thus, it is not important *that* oscillations can be obtained. The important question is: are conditions and results *in fact applicable* to natural samples that have been positively identified to be kinetically controlled? It is of little value to apply existing kinetic models to explain STR-oscillations. Our LAO patterns may be an appropriate candidate for kinetically controlled oscillations. The wavelength ranges between 1–20 μm and the amplitude is 0.5–2 mol% An. The profile shape, which is, unfortunately, not well defined, shows no clear asymmetry. Thus, we discuss here the relevance of the existing models to the observed LAO oscillations, which may be kinetically controlled.

Existing numerical models mainly differ by the assumption on partitioning of Ab and An components between melt and crystal under non-equilibrium conditions. Some models assume that the growing crystal is in equilibrium with the adjacent melt. A general solution for the growth equations in these conditions is given by Lasaga (1982). With such assumptions, L'Heureux and Fowler (1994, 1996a, 1996b) obtained oscillations in their models. However, the resulting amplitudes and wavelengths are too high (≥10 mol% An, ≥40 μm). Furthermore, their models needs particular conditions on the partition coefficient of anorthite. The conditions described in L'Heureux and Fowler (1994) only occur in plagioclase with An ≤50. In L'Heureux and Fowler (1996a, 1996b), the parameter K_D, which must be smaller than 1 in order to produce oscillations is, in fact, $K_D = (c^s_{An})/c^l_{An})/(c^s_{Ab}/c^l_{Ab})$ where the superscripts *s* and *l* respectively refer to the solid and the liquid. In local equilibrium, this K_D is always larger than 1, so this model fails to produce oscillations under realistic conditions.

Other models (Haase et al. 1980; Ortoleva 1990; Wang and Wu 1995) consider that the partitioning between Ab and An is controlled by the interface attachment kinetics of both components, which, in turn, depend on the composition of the existing crystal. The oscillations obtained also have amplitudes that are too high (40 to 80 mol% An) and asymmetric saw-tooth profiles with sharp peaks that do not match the observed LAO profiles. Adding small random variations in An-concentration in the melt far from the crystal does not influence the amplitude of the resulting variations (Holten et al. 2000).

Pearce (1994) proposed a phenomenological numerical model based on the idea of Sibley et al. (1976). He assumed that growth occurs with a constant partition coefficient, but only if the supersaturation in the melt exceeds a certain value. This model produces saw-tooth patterns at high growth rates, however, they do not involve resorption. No small-scale symmetrical oscillations are reported in the results, but the model was not designed to produce this type of oscillation.

The model of Allègre et al. (1981) also uses a phenomenological approach to explain oscillations. They assume a delay in the response that the growth rate gives to a change in the liquid concentration at the interface, and they introduce an additional differential equation to describe it. The regular steady-state solution is similar to that of Lasaga (1982). Superimposed smooth asymmetrical damped oscillations are obtained through perturbations of small amplitude. The amplitude of oscillations is that of the initial small perturbation and the wavelength is not constrained by the model. A low damping factor is favored by low degrees of supersaturation. The resulting oscillations may be comparable to our observations. However, because it is a phenomenological model, several parameters (wavelength, amplitude) are not constrained. Theoretical and experimental constraints are needed to assess whether the mechanism (delay in the response of growth rate to liquid concentration) really occurs in natural magmas.

An additional model (Anderson 1984) for oscillatory zoning proposes a combination of kinetic and dynamic models. In a supersaturated liquid, a local boundary layer is formed at the crystal–melt interface. It is assumed that the growing crystal is in equilibrium with the melt composition regardless of temperature. The periodic destruction of the boundary layer, caused by a shear pulse caused by the effect of tides on pressure, brings more supersaturated melt to the crystal surface. The resulting new plagioclase grows from a more mafic composition and is thus more calcic. However, the growth rate needed to grow one 1- to 20-μm-wide zone per day is approximately 10^{-9} to 2. 10^{-8} cm/s, which is much faster than the generally accepted although poorly constrained 10^{-10} to 10^{-11} cm/s (Cashman 1990). Furthermore, the assumption of equilibrium composition in the growing crystal still has to be verified.

In conclusion none on the existing kinetic models satisfy the observed small amplitude oscillations: some of them (L'Heureux and Fowler 1994, 1996a, 1996b; Haase et al. 1980; Ortoleva 1990; Wang and Wu 1995) are ruled out by the scale and amplitude of the oscillations whereas, two others (Allègre et al. 1981; Anderson 1984) may be plausible but are too poorly constrained.

Inverse zoning patterns and kinetics

Another model that combines kinetics and small-scale dynamics is that of Loomis (1982). In contrast to the model of Anderson (1984), Loomis (1982) assumes that the growing plagioclase has the solidus composition at the temperature considered. Water rejected in the boundary layer during crystal growth plays a dominant role: it locally reduces the liquidus and solidus temper-

atures together with local undercooling and, thus, increases the An content in the growing crystal. Such a process could explain the rare inverse zones found in the PAR-130-P3. An initial supersaturation could be caused by an external cause, such as the disturbance of an existing water-rich boundary layer, or temperature drop, degassing, etc. Inverse zoning then occurs when the system comes back to equilibrium through the local chemical evolution of the melt because of crystallization. The width of the inverse zones in Loomis' model (50–200 μm) is, however, larger than the 10-μm-wide inverse zones observed in our sample.

It should be noted that this model is neither compatible with that of Anderson (1984), nor with that of Allègre et al. (1981) because it assumes a different partitioning law at the crystal interface. More experimental data are needed to determine the actual partitioning law in disequilibrium growth.

Conclusion

High quality accumulated BSE images, which are possible with the new generation of electron microprobes, provide a major improvement in imaging and analysis of major element zoning in plagioclase. This makes more accurate quantification of small-scale zoning patterns possible.

Our observations show at least two types of oscillatory zoning at scales smaller than 20 μm, 5–10 mol% An, which both correspond to the type I oscillations of Pearce and Kolisnik (1990). This indicates that higher resolution imaging allows for a better distinction of oscillatory zoning types. STR patterns are non-periodic saw-tooth-shaped "oscillations" characterized by resorption surfaces. We attribute this type of oscillations to dynamic processes such as (turbulent) convection, which includes resorption phases, as assumed for the type II oscillations of Pearce and Kolisnik (1990). Only LAO patterns (amplitude $< 2\%$ An) may be true oscillations caused by a kinetic effect. They are also found in a plagioclase crystal derived from a cumulate. Among the existing models, that of Allègre et al. (1981) is closest to these particular oscillations, but needs to be better tested for its applicability if magmatic parameters and conditions are to be extracted.

The oscillations described here are representative for the sample studied. However, it can not be excluded that the characteristics (amplitude and wavelength) of both types of oscillations vary in other systems (different melt composition, magma chamber dynamics, etc.), or even that other types exist that have yet to be recognized. A systematic study using accumulated BSE images of plagioclase in a large range of systems (volcanics to cumulates and various compositions) should allow us to generalize the different types of oscillatory zoning and the different processes that produce them.

Acknowledgements We would like to thank George Bergantz for stimulating discussions and helpful comments on a early version of the manuscript. Two anonymous reviewers provided valuable input through constructive comments. This study was part of the DFG-funded SFB 468.

Appendix: An-calibrated accumulated BSE images

Principle

Backscattered electrons are emitted close to the surface of the sample: The sampling depth depends on the mean atomic number of the material and is ≤ 1 μm for feldspars (Goldstein et al. 1992). The emission intensity of BSE depends mainly upon the mean atomic number of the sample. In plagioclase, this is related to the Ca/Na ratio and thus to An content. The influence of K content is discussed later. Other elements, such as Fe, Ba, and Sr have variations of at most a few hundred ppm in the investigated plagioclase crystals (Ginibre et al. 2001) and, therefore, cannot significantly affect BSE intensity.

Other effects may influence the BSE signal. For example, electron channeling affects BSE intensity depending on crystal lattice orientation independently from compositional variations. This is a common problem in plagioclase because of polysynthetic twins. However, this artifact can be readily recognized and avoided by careful choice of the crystal section. Artifacts caused by an imperfect surface polish are randomly oriented and add to the statistical noise. They are generally small compared with the An signal but become more important in low contrast images as shown in Fig. 2a (LS-15616-P1). Irregularities in carbon coating, especially as a result of quantitative analysis spots are also seen in BSE and, therefore, images must be acquired prior to quantitative point analysis.

Spatial resolution of the BSE signal depends mainly on the sampling volume of BSE. The backscattered intensity may be calculated as a function of the distance from the beam impact point (Goldstein et al. 1992). This represents a transfer function of the BSE signal, which will be convoluted with the initial compositional information to give the resulting image. For the mean atomic number of feldspar, the radius within which 80–90% of BSE intensity is emitted, is about 1 μm at 15 kV acceleration voltage. In a more practical sense, the spatial resolution is the minimum distance at which two zones of different composition are seen. However, this spatial resolution depends on the contrast and is, therefore, not independent of the compositional resolution. On the basis of the finest observed zones, spatial resolution is estimated to be 0.5 μm in PAR-130-P1 for contrasts of 1–2 mol% An (see below). Near the limit of resolution, the profile is smoothed by the transfer-function of the BSE signal.

Image acquisition

Particular attention was given to obtaining a high-quality polish of the thin sections because the state of the surface has a large influence on the quality of the images.

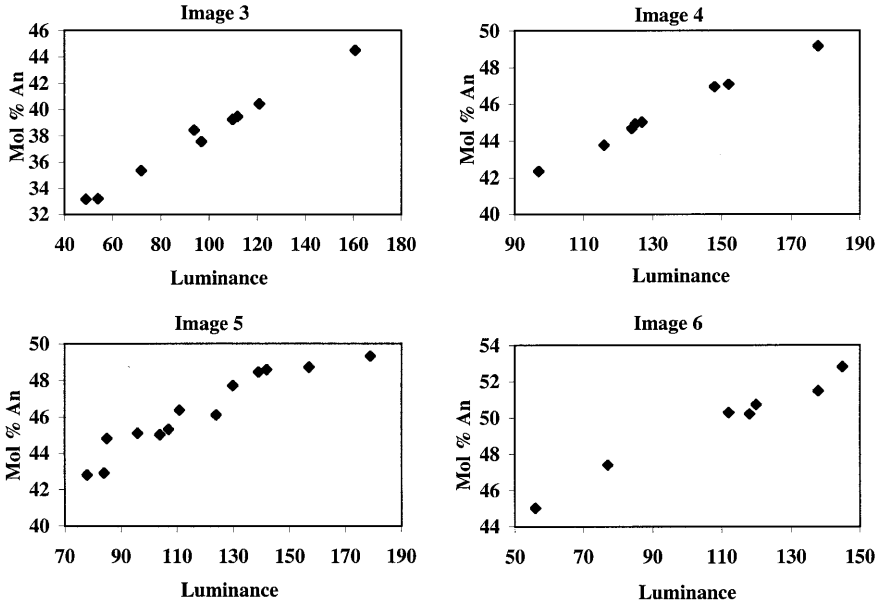

Fig. 6 Calibration lines for four accumulated BSE images of PAR 130-P3: anorthite content from the quantitative analyses is plotted against the luminance of the corresponding points on the images. It can be seen that the quality of the correlation varies between different images

An acceleration voltage of 15 kV and a beam current of 20 nA were used for all images. By accumulating 10–30 BSE images of the same part of the sample, a higher signal/background ratio was obtained. This increases the compositional resolution.

Gray scale profiles

Gray scale (or luminance) profiles normal to planar growth zones are measured on the accumulated BSE images using image analysis software (Optimas). Each point of the profile represents the luminance averaged on a sampling area. For each image, width (normal to the profile direction) and length (parallel to the profile direction) of the sampling units are chosen to be large enough to reduce noise, but small enough not to average different compositions. They thus depend on the width and lateral variability of the growth zones. We chose sampling areas of 100 pixels (width)×5 pixels (length) for the image of the Laacher See cumulate feldspar (15616) and of 8 pixels (width)×3 pixels (length) for all images of PAR-130-P3.

Calibration

The measuring points of quantitative analysis are seen on subsequent simple BSE images and thus can be located precisely on the accumulated BSE images. Image analysis is then performed as for the profile. For the calibration, the luminance was averaged over the area corresponding to each measurement point, which has a diameter of 5 or 2 μm. This allows us to take into account the different lateral spatial resolutions of EMP quantitative analyses and the BSE signal. For some measurements points located on a zone boundary, the result of gray scale determination is very sensitive to the exact positioning of the sampling area on the image. Such points were excluded from the calibration.

Measured luminance of quantitative measurement points are plotted against An content for each image and are shown in Fig. 6 for four images of PAR-130-P3. There is a good linear correlation between the individual quantitative point analyses (10 to 15 points) and BSE gray scale (luminance) measured on the image at the same spot. Each image is individually calibrated for An content using the determined linear correlation. An-calibrated profiles over the entire crystal from core to rim are then obtained by combining individual calibrated gray scale profiles.

The effect of K_2O concentration is accounted for in the linear calibration because the K_2O content is almost linear with An in the compositional range of one image. As is seen in Fig. 6, the quality of the correlation varies between the images. This is explained as follows: in contrast to lateral variations, differences in sampling depth between BSE signal and quantitative analysis can not be corrected for. They are generally small because growth zones are almost normal to the section, but the effect is larger when zone boundaries are wavy. This effect is the most important source of uncertainty in the calibration. The images with the poorest correlation are those with wavy boundaries (image 5).

Precision and accuracy

The precision of the An-calibrated profile is the compositional resolution and depends only on the quality of the BSE images and gray scale profiles and not on the calibration. Figure 2 compares three parallel profiles from the image of LS15616 and shows that, despite polishing artifacts, they differ by less than 0.5 mol% An

from each other. Structures with 0.5 mol% An amplitude are recognized on the three profiles and are well correlated. On the images of PAR-130-P3 (Fig. 4), the precision of the profiles is slightly lower (1% An) because of the higher lateral variability and smaller width of zones ($\leq$1 μm). However, at small An variations, real compositional zones (parallel to the growth surface) can be distinguished from artifacts or statistical noise by direct comparison of the profiles with the corresponding BSE image.

By contrast, the accuracy of the An-calibrated profiles depends upon the quality of the calibration line. This is controlled by the precision and accuracy of the quantitative analyses and by the difficulty of comparing BSE signal and quantitative analyses, as discussed above. The resulting accuracy is not better than a few mol% An. However, the important point in our study is the precision and the relative compositional variations in the profiles, and not the absolute values for An.

When analyzing the profiles, it should be noted that the lateral variations of single zones are often larger than the uncertainty caused by the calibration or the precision of the BSE-signal. Another point to keep in mind is that the observed signal is not necessarily the initial composition at the time of crystallization because of the possibility of late diffusive equilibration. Its effect on a profile of any shape would be a relaxation towards a sinusoid curve (Shore and Fowler 1996). This effect is expected to be small for large wavelengths (Grove et al. 1984), and, indeed, observed variations at the 10–100-μm-scale are often asymmetrical and not sinusoidal. However, diffusion may have affected smaller features ($\leq$1 μm). The profile observed is therefore smoothed with respect to the initial zoning pattern by two phenomena: naturally through diffusion, and analytically through a transfer function of BSE emission. This means that transitions in reality may be sharper than actually seen in the images and the An-calibrated BSE gray scale profiles.

References

Allègre CJ, Provost A, Jaupart C (1981) Oscillatory zoning: a pathological case of crystal growth. Nature 294:223–228

Anderson AT Jr (1983) Oscillatory zoning of plagioclase: Nomarski interference contrast microscopy of etched polished sections. Am Mineral 68:125–129

Anderson AT (1984) Probable relations between plagioclase zoning and magma dynamics, Fuego Volcano, Guatemala. Am Mineral 69:660–676

Baronnet A (1984) Growth kinetics of the silicates – a review of basic concepts. Fortschr Miner 62:187–232

Berndt J, Holtz F, Koepke J (2001) Experimental constraints on storage condition in the chemically zoned phonolitic magma chamber of the Laacher See volcano. Contrib Mineral Petrol 140:469–486

Blundy JD, Shimizu N (1991) Trace element evidence for plagioclase recycling in calc-alkaline magmas. Earth Planet Sci Lett 102:178–197

Bogaard P (1995) ^{40}Ar–^{39}Ar ages of sanidine phenocrysts from Laacher See Tephra (12.900 yr B.P.): chronostratigraphic and petrological significance. Earth Planet Sci Lett 133:163–174

Bottinga Y, Kudo A, Weill D (1966) Some observations on oscillatory zoning and crystallization of magmatic plagioclase. Am Mineral 51:792–806

Bourdon B, Zindler A, Wörner G (1994) Evolution of the Laacher See magma chamber: evidence from SIMS and TIMS measurement of U–Th desequilibria in minerals and glasses. Earth Planet Sci Lett 126:75–94

Brophy JG, Dorais MJ, Donnelly-Nolan J, Singer B (1996) Plagioclase zonation in Hornblende gabbro inclusions from Little Glass Mountain, Medicine Lake volcano, California: implications for fractionation mechanisms and the formation of composition gaps. Contrib Mineral Petrol 126:121–136

Cashman KV (1990) Textural constraints on the kinetics of crystallization of igneous rocks. In: Nicholls J, Russell JK (eds) Reviews in mineralogy, vol 24. Modern methods of igneous petrology, understanding magmatic processes. Mineral Soc Am, Washington, DC, pp 259–314

Davidson JP, Tepley FJ (1997) Recharge in volcanic system: evidence from isotope profiles of phenocrysts. Science 275:826–829

Davidson JP, McMillan NJ, Moorbath S, Wörner G, Harmon RS, Lopez-Escobar L (1990) The Nevados Payachatas volcanic region (18°S/69°W, N. Chile) II. Evidence for widespread crustal involvement in Andean magmatism. Contrib Mineral Petrol 105:412–432

Ginibre C, Wörner G, Kronz A (2001) Minor and trace element zoning patterns in volcanic plagioclase: crystal–chemical, compositional and kinetic control and implications for magma chamber processes. Contrib Mineral Petrol (in press)

Goldstein JI, Newbury DE, Echlin P, Joy DC, Roming AD Jr, Lyman CEC, Lifshin E (1992) Scanning electron microscopy and X-ray analysis. A text for biologists, material scientists and Geologists, 2nd edn. Plenum Press, New York

Grove TL, Baker MB, Kinzler RJ (1984) Coupled CaAl–NaSi diffusion in plagioclase feldspar: experiments and application to cooling rate speedometry. Geochim Cosmochim Acta 58:2113–2121

Haase CS, Chadam J, Feinn D, Ortoleva P (1980) Oscillatory zoning in plagioclase feldspar. Science 209:272–274

Hammouda T, Pichavant M (2000) Melting of fluorophlogopite–plagioclase pairs at 1 atmosphere. Eur J Mineral 12:315–328

Harms E, Schmicke HU (2000) Volatile composition of the phonolitic Laacher See magma (12,900 yr B.P.): implications fro the syn-eruptive degassing of S, F, Cl and H_2O. Contrib Mineral Petrol 138:84–98

Holten T, Jamveit B, Meakin P (2000) Noise and oscillatory zoning in minerals. Geochim Cosmochim Acta 64:1893–1904

Homma F (1932) Über das Ergebnis von Messungen an zonaren Plagioklasen aus Andesiten mit Hilfe des Universaldrehtisches. Schweizer Mineral Petrogr Mitt 12:345–351

Housh TB, Luhr JF (1991) Plagioclase – melt equilibria in hydrous system. Am Mineral 76:477–492

Johannes W (1978) Melting of plagioclase in the system Ab–An–H_2O at $P_{H2O} \leq 5$ kbars, an equilibrium problem. Contrib Mineral Petrol 66:295–303

Johannes W, Koepke J, Behrens H (1994) Partial melting reactions of plagioclases and plagioclase bearing systems. In: Parson I (ed) Feldspars and their reactions. Kluwer, Dordrecht, pp 161–194

Kirkpatrick RJ (1981) Kinetics of crystallization of igneous rocks. In: Lasaga AC, Kirkpatrick RJ (eds) Reviews in mineralogy, vol 8. Kinetics of geological processes. Mineral Soc Am, Washington, DC, pp 321–398

Kirkpatrick RJ, Klein LM, Uhlman DR, Hays JF (1979) Rates of and processes of crystal growth in the system anorthite–albite. J Geophys Res 84:3671–3676

Kuo LC, Kirkpatrick RJ (1982) Pre-eruption history of phyric basalts from DSDP legs 45 and 46: evidences from morphology

and zoning patterns in plagioclase. Contrib Mineral Petrol 79:13–27
Kuritani T (1998) Boundary layer crystallization in a basaltic magma chamber: evidence from Rishiri Volcano, northern Japan. J Petrol 39:1619–1640
Lasaga AC (1982) Toward a master equation in crystal growth. Am J Sci 282:1264–1288
L'Heureux I, Fowler AD (1994) A nonlinear dynamical model of oscillatory zoning in plagioclase. Am Mineral 79:885–891
L'Heureux I, Fowler AD (1996a) Isothermal constitutive undercooling as a model for oscillatory zoning in plagioclase. Can Mineral 34:1137–1147
L'Heureux I, Fowler AD (1996b) Dynamical model of oscillatory zoning with non linear partition relation. Geophys Res Lett 23:17–20
Lofgren GE (1974) An experimental study of plagioclase crystal morphology: isothermal crystallization. Am J Sci 274:243–273
Lofgren GE (1980) Experimental studies on the dynamic crystallisation of silicate melts, ch 11. In: Hargraves RB (ed) Physics of magmatic processes. Princeton University Press, Princeton
Loomis TP (1982) Numerical simulations of crystallization processes of plagioclase in complex melts: the origin of major and oscillatory zoning in plagioclase. Contrib Mineral Petrol 81:219–229
Loomis TP, Welber PW (1982) Crystallization processes in the Rocky Hill granodiorite pluton, California: an interpretation based on compositional zoning of plagioclase. Contrib Mineral Petrol 81:230–239
Marsh BD (1989) Magma chambers. Annu Rev Earth Planet Sci 17:439–474
Muncill GE, Lasaga AC (1987) Crystal growth kinetics of plagioclase in igneous systems: one-atmosphere experiments and application of a simplified growth model. Am Mineral 72:299–311
Muncill GE, Lasaga AC (1988) Crystal growth kinetics of plagioclase in igneous systems: isothermal H_2O-saturated experiments and extension of a growth model to complex silicate melts. Am Mineral 73:982–992
Nakamura M, Shimakita S (1998) Dissolution origin and syn-entrapment compositional changes of melt inclusions in plagioclase. Earth Planet Sci Lett 161:119–133
Nixon GT, Pearce TH (1987) Laser-interferometry study of oscillatory zoning in plagioclase: the record of magma mixing and phenocryst recycling in calc-alkaline magma chambers, Iztaccíhuatl volcano, Mexico. Am Mineral 72:1144–1162
Ortoleva PJ (1990) Role of attachment kinetic feedback in the oscillatory zoning of crystals grown from melts. Earth Sci Rev 29:3–8
Pearce TH (1994) Recent work on oscillatory zoning in plagioclase. In: Parson I (ed) Feldspars and their reactions. Kluwer, Dordrecht, pp 313–349
Pearce TH, Kolisnik AM (1990) Observation of plagioclase zoning using interference imaging. Earth Sci Rev 29:9–26
Pearce TH, Russel JK, Wolfson I (1987) Laser-interference and Nomarski interference imaging of zoning profiles in plagioclase phenocrysts from the May 18 1980, eruption of Mount St. Helens, Washington. Am Mineral 72:1131–1143
Shore M, Fowler AD (1996) Oscillatory zoning in minerals: a common phenomenon. Can Mineral 34:1111–1126
Sibley DF, Vogel TA, Walker BM, Byerly G (1976) The origin of oscillatory zoning in plagioclase: a diffusion and growth controlled model. Am J Sci 276:275–284
Singer B, Dungan MA, Layne GD (1995) Textures and Sr, Ba, Mg, Fe, K, and Ti compositional profiles in volcanic plagioclase: clues to the dynamics of calc-alkaline magma chambers. Am Mineral 80:776–798
Smith J, Brown WL (1988) Feldspar minerals: I crystal structures, physical, chemical and microtextural properties, 2nd edn. Springer, Berlin Heidelberg New York
Smith RK, Lofgren GE (1983) An analytical and experimental study of zoning in plagioclase. Lithos 16:153–168
Tait SR (1988) Samples from crystallizing boundary layer of a zoned magma chamber. Contrib Mineral Petrol 100:470–783
Tait SR, Wörner G, Bogaard Pvd., Schmincke H-U (1989) Cumulate nodules as evidence for convective fractionation in a phonolite magma chamber. J Volcanol Geotherm Res 37:21–37
Tsuchiyama A (1985) Dissolution kinetics of plagioclase in the melt of system diopside–albite–anorthite, and origin of dusty plagioclase in andesites. Contrib Mineral Petrol 89:1–16
Wang JH, Wu JP (1995) Oscillatory zonation of minerals and self-organization in silicate solid-solution systems: a new nonlinear dynamic model. Eur J Mineral 7:1089–1100
Wiebe RA (1968) Plagioclase stratigraphy: a record of magmatic conditions and events in a granite stock. Am J Sci 266:690–703
Wörner G, Schmincke HU (1984a) Mineralogical and chemical zonation of the Laacher See Tephra Sequence (East Eifel, W Germany). J Petrol 25:805–835
Wörner G, Wright TL (1984). Evidence for magma mixing within the Laacher See Magma chamber (East Eifel, Germany). J Volcanol Geotherm Res 22:301–327
Wörner G, Harmon RS, Davidson J, Moorbath S, Turner DL, McMillan N, Nye C, Lopez-Escobar L, Moreno H (1988) The Nevados de Payachata volcanic region (18°S/69°W, N. Chile): I. Geological, geochemical, and isotopic observations. Bull Volcanol 50:287–303
Wörner G, Hammerschmidt K, Henjes-Kunst F, Lezaun J, Wilke H (2000) Geochronology ($^{40}Ar/^{39}Ar$, K–Ar and He-exposure ages) of Cenozoic magmatic rocks from northern Chile (18–22°S): implication for magmatism and tectonic evolution of the central Andes. Rev Geol Chile 27:205–240
Yoder HS, Stewart DB, Smith JR (1957) Ternary feldspars. Carnegie Institute of Washington Yearbook, vol 56, pp 206–214